International Journal of Environmental Sciences
ISSN: 2229-7359
Vol. 11 No. 24s, 2025
https://www.theaspd.com/ijes.php

A Novel Method For Corona Discharge Detection Under Low-Pressure Conditions Using Laser Speckle Pattern

Krishanlal Adhikari, C. Koley, Nirmal Kumar Roy

***Abstract*–** *Monitoring the insulation condition is essential for the efficient functioning of any electrical apparatus. Deterioration of the insulation is predominantly caused by various operational stresses at harsh environmental conditions that lead to electrical discharges. Corona discharge is a common and crucial phenomenon in electrical apparatus. Corona discharge detection is considered an essential predictive maintenance method that ensures the sound operation of electrical equipment. Discharge activities significantly depend on pressure conditions and pose a risk to electrical equipment working under low pressure. This paper proposes an acousto-optic effect-based novel, noninvasive method of corona detection where corona discharge is emulated in a laboratory-based setup under low-pressure conditions and detected using the proposed and conventional IEC 60270-based methods simultaneously. It is observed that the increment in the discharge magnitude and repetition rate, as suggested by the phase-resolved discharge analysis obtained from the conventional method, is correlated with the change in the shape of the speckle pattern and the intensity of the speckle grain. Hence, the above methodology can be used as a new tool for analyzing the discharges of electrical power apparatus, especially installed in low-pressure environments such as aircraft operating in high altitudes. Later, for simplification and real-time applications, the above-mentioned experiment is conducted using an optical fiber-based model where two optical fibers forming a fiber-to-fiber coupling through air are developed, and the modulation of the coupled light by the corona discharge-generated acoustic wave is observed. The outcomes establish that the proposed method detects corona discharge reliably, and the sensitivity of detection is comparable with the standard IEC 60270-based method, with a noninvasive, cost-effective, and all-dielectric approach.*

***Index Terms*–** *Acousto-optic effect, condition monitoring, corona discharge, laser speckle pattern, low-pressure conditions.*

I. INTRODUCTION

INSULATION deterioration in any electrical power apparatus is predominantly caused by electrical, thermal, chemical, mechanical, and environmental aging [1]. Aging of the insulation leads to the formation of weak points that are susceptible to electrical discharges, and the detection of electrical discharges is a well-accepted predictive maintenance tool to assess the health of the insulation [2]. The electrical discharges can be classified into three major categories [3], i.e., corona discharge, surface discharge, and internal discharge. Among them, corona discharge is recognized as the most common type of electrical discharge that often takes place in close proximity to sharp metal edges where the electrical field is highly inhomogeneous [4]. It is also understood from several studies that the corona discharge inception voltage is susceptible to environmental pressure, as corona incepts at a lower voltage in low atmospheric pressure conditions [5], [6]. It creates local hotspots [7] and liberates ozone gas, which expedites the oxidation of dielectric materials [8] and accelerates the degradation of the insulation. Consequently, detecting the corona discharge at its nascent stages is crucial for the reliable operation of any electrical power apparatus operating in adverse environmental conditions.

There are different types of conventional and sensor-based methods for the detection of corona discharges, i.e., Electrical, Electromagnetic, Acoustic, and Optical. The IEC 60270-based electrical PD detection method is the standard laboratory-based offline method for the detection of partial discharge. This method requires direct contact between the test object and the bulky coupling capacitor, so using this method online monitoring is not feasible [9]. Electromagnetic detection using different types of antennas is a popular method, but the high cost associated with the data acquisition system, along with the complexity of high-frequency wideband sensor design, limits the practicality of this technique [10]. Acoustic detection is a cost-effective and efficient technique with a potential scope of online and onsite installation, but suffers from a low signal-to-noise ratio [11]. Optical detection using optical fiber sensors is an effective method as it is immune to electromagnetic interference (EMI), highly sensitive, and offers a wideband frequency spectrum. Still, some major disadvantages, like the involvement of the complex and sophisticated sensor design and costly interrogating systems, limit its applicability [12].

Many non-conventional corona detection techniques have been proposed recently, assimilating high sensitivity, remote sensing capability, and the scope of online and onsite real-time monitoring. Ultraviolet (UV) detection-based corona camera utilizes ultraviolet imaging to detect, quantify, and locate the characteristic glow emitted by corona discharge, enabling highly reliable monitoring of corona events at any electrical infrastructure. [13] proposes an innovative scheme for insulation monitoring and criticality classification based on a UV detection camera-based dataset. A limitation of UV camera-based corona detection is its susceptibility to interference from ambient light, potentially leading to inaccuracies in detecting corona discharges. Additionally, UV cameras exhibit a limited range with line of sight detection, diminished distance sensitivity, vulnerability to adverse environments, limited spectral information, and inadequate calibration technique that limits the practical applications.

Acoustic microphone-based ultrasonic corona imaging techniques offer another non-conventional method for corona detection, capturing the acoustic emissions produced by corona discharge. Specialized microphones detect the distinct sound signatures associated with corona activities. This approach allows for real-time monitoring of corona events, even in challenging environmental conditions. [14] established the basic ultrasonic imaging technique, considering distance, frequency, temperature, and humidity, and identified essential environmental conditions for corona detection through repeated measurements. Acoustic microphone-based corona discharge detection may be hindered by susceptibility to background noise, potentially leading to false alarms or missed detections, limited range, low spectral bandwidth, etc. A study presented in [15] evaluates three low-cost corona detection methods under low-pressure environments (10–100 kPa), i.e., loop antenna, visible-UV imaging, and leakage current measurement, where all methods showed stable, linear responses, with UV imaging offering source localization despite slightly lower sensitivity. [16] demonstrates low-cost CMOS visible-UV imaging for detecting and locating corona in aeronautic environments, equivalent environments, and achieves an accurate, sensitive, as well as affordable detection, helping prevent arc tracking.

In addition to the above, other innovative sensors are popularly used for corona detection as well, utilizing principles such as fluorescence spectroscopy [17], optical spectrophotometers [18], and sound level meters [19]. Fluorescence-based sensors detect the emission of ultraviolet light produced during corona discharge, while optoacoustic sensors measure the acoustic waves emitted by the rapid heating and expansion of the medium in the vicinity of corona discharge.

In practical fields such as aircraft engineering, where HV equipment works at considerably low pressure, understanding the behavior of corona discharge under low pressure is crucial for ensuring the safety and reliability. In order to increase efficiency and sustainability, next-generation aircraft are heading towards environment-friendly All-Electric Aircraft (AEA). Such aircraft use higher voltage electrical distribution systems to accommodate the increasing power demand while lowering system weight, which raises the

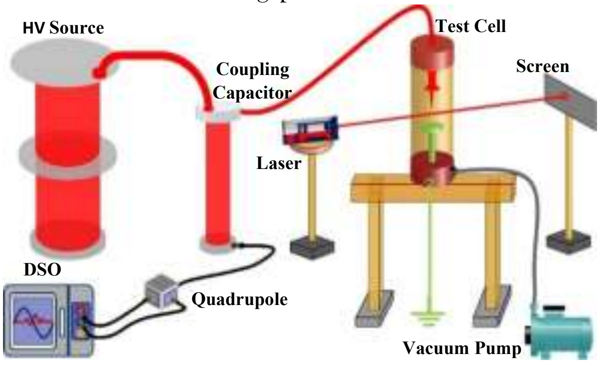

risk of corona

Fig.1. Schematic of Experimental Setup

discharge invoked by low-pressure situations during flying. Low-pressure situation is crucial for insulation reliability since pressure significantly lowers the inception of corona discharge.

It motivates the researchers to design sensitive and reliable condition monitoring systems for insulation to address challenges posed by low-pressure environments.

This paper introduces a novel corona discharge detection system under low-pressure conditions, using laser speckle patterns and the acousto-optic effect induced by acoustic waves from corona discharges.. This proposed approach ensures better sensitivity and reliable detection of insulation degradation, crucial for maintaining the integrity and reliability of the electrical infrastructure. In this work, variations in light patterns by the acoustic wave evolving from corona discharges are captured through the laser speckle pattern analysis. The proposed method enables real-time monitoring of corona activities, aiding in early fault detection and preventing the failure of an electrical infrastructure. By establishing the relation between laser speckle analysis and acousto-optic phenomena, the proposed work presents a promising advancement in corona detection technology for the energy sector. The major contribution of the work is as follows.

1) It introduces an innovative approach utilizing laser speckle patterns for corona detection at different voltage levels, offering a reliable and non-intrusive method suited for low-pressure conditions such as aircraft operating in high altitudes, where traditional detection methods may prove inadequate.

2) An optical fiber-based model is proposed based on the above methodology, comprising an air-coupled single-mode fiber (SMF) to SMF coupling, which is designed and developed for near-field monitoring of Corona discharge in HV equipment.

The rest of the paper is organized as follows: Section II explains the fundamental principle of laser speckle pattern-based corona detection with governing equations, Section III describes the methodology and experimental setup, Section IV deals with the results and relevant discussions, and Section V concludes the work.

II. THEORY OF LASER SPECKLE PATTERN-BASED CORONA DETECTION

The acousto-optic effect is the physical effect that happens when acoustic waves propagate through a medium and change its refractive index. When corona discharge happens in electrical systems, it creates acoustic waves that travel through the surrounding medium and change the medium density and pressure in specific areas. Changes in the density and pressure of the medium cause the refractive index of the medium to change along the propagation path of the acoustic waves. Thus, the acousto-optic effect alters the refractive index of the medium, which in turn modifies the length of the optical path experienced by the laser light passing by the affected area. This change in the optical path length causes the light waves to shift in phase, which then changes the interference pattern seen on a screen as a laser speckle pattern. A photodetector can also monitor this change in the intensity of the laser light.

Partial discharges (PD) in dielectric media release fast pressure transients that generate localized acoustic waves. These acoustic fields interact with photons traversing the medium and modulate the transmitted laser light. In the mechanisms, both refractive index variation and scatterer displacement lead to measurable changes in light intensity.

The phase change induced by refractive index variation along the *i*-th free path is presented in (1)

$$\theta_{ni}(t) = \int_0^{l_i} u_0 \Delta n(\vec{r}_{i-1,} s_{i,} \alpha_{i,} t)\, ds_i \qquad (1)$$

The phase shift $(\theta_{ni}(t))$ is obtained by integrating the product of the optical wavenumber (u_0) and the ultrasound-induced refractive index perturbation (Δn) along the i-th scattering path of length l_i. The refractive index perturbation depends on the scatterer's position $(\vec{r}_{i-1})$, the fractional distance (s_i), the propagation angle (α_i) between ultrasound and optical vectors, and time t.

The refractive index perturbation at position $\vec{r}$ and time t is related to the PD acoustic field by (2), where m_0 is the unperturbed refractive index of the medium, η is the pressure–index coupling constant, M is the acoustic amplitude, v_a and ω_a the acoustic wavenumber and frequency, $\overrightarrow{k_a}$ is the acoustic

$$\begin{cases} \Delta n(\vec{r}, t) = m_0 \eta v_a M \sin(\overrightarrow{k_a}.\vec{r} - \omega_a t) \\ \eta = (\partial n / \partial p) \text{þ} u_a^2 \end{cases} \qquad (2)$$

wave vector, p is acoustic pressure, u_a denotes the acoustic velocity and þ represents medium density. Combining refractive index and scatterer displacement effects, the autocorrelation $(\mathrm{G}(\tau))$ of the optical field becomes (3).

$$\mathrm{G}(\tau) = \int_0^{\infty} g(s) exp\left\{-\frac{2s}{l}(\delta_n + \delta_d)[1 - \cos(\omega_a \tau)]\right\} ds \qquad (3)$$

where $g(s)$ is the probability density function of photon path length s, l is the optical transport mean free path, τ is the temporal lag in the autocorrelation function, δ_n and δ_d present the contributions from the refractive index and scatterer displacement. The detected intensity at the acoustic sidebands can then be obtained via the Wiener–Khinchin theorem as presented in (4).

$$I_n = \frac{1}{T}\int_0^{T} \mathrm{G}(\tau) \cos(n\omega_a \tau)\, d\tau \qquad (4)$$

Where n is the harmonic order and T the acoustic period, thus, corona-generated acoustic waves impose periodic phase shifts that accumulate along photon paths, leading to temporal modulation of detected laser light intensity. Therefore, the speckle patterns are closely related to the acoustic optic effect, due to the interaction of coherent light with acoustic waves. The modulation of laser light properties with corona discharges can be visualized and measured with the speckle grain intensity and pattern change or interrogated by a suitable photodetector.

Hence, the corona discharge detection by laser speckle pattern analysis is an innovative approach that provides information regarding local ionization events caused by discharges, as the speckle intensity near the discharge site changes with voltage and pressure. By analyzing these changes in the speckle pattern, or the intensity modulation of the intercepted signal from the photodiode, it is possible to detect and characterize corona discharge events, offering a reliable method for detecting and monitoring corona discharge in any electrical infrastructure.

III. Experimental Setup

The experimental investigations were carried out at the high voltage laboratory in two parts, i.e., observing the variation in laser speckle pattern due to emulated corona discharges under NTP as well as lower atmospheric pressure, and detection of corona discharge at NTP by the developed optical fiber model comprising SMF-SMF coupling in air. In the first part, to access the reliability, the emulated corona discharge events are monitored simultaneously by a standard IEC 60270-based partial discharge (PD) detection unit and laser speckle–based optical sensing arrangement.

In the conventional PD detection system, a high-voltage test transformer rated at 0–300 kV, 50 Hz, .05A was employed as the excitation source. The secondary of the source transformer is connected to the needle-flat electrode arrangement as a PD source kept inside a variable pressure chamber via a coupling capacitor of 300 pF, rated voltage of 300 kV, as shown in Fig. 2. The coupling capacitor was connected in parallel to the electrode arrangement. A quadrupole (AVK-D), with impedance matching and filtering circuit, is employed for the data acquisition using the standard method. The output of the quadrupole was connected to a conventional PD detection unit and a digital storage oscilloscope (Tektronix, 500 MHz bandwidth, 2.5 GS/s) for monitoring as well as recording the acquired discharge events. The AC phase reference data was collected from the low-voltage terminal of the resistive divider of the source transformer to allow synchronization of the PD signals with the sinusoidal excitation for phase-resolved analysis. To identify the phased resolved partial discharge (PRPD) from the standard method, each discharge pulse is referenced to the phase angle of the applied AC voltage, allowing time–phase synchronization. Accumulated over cycles, these events form PRPD plots that reveal discharge magnitude and phase distribution for insulation diagnosis.

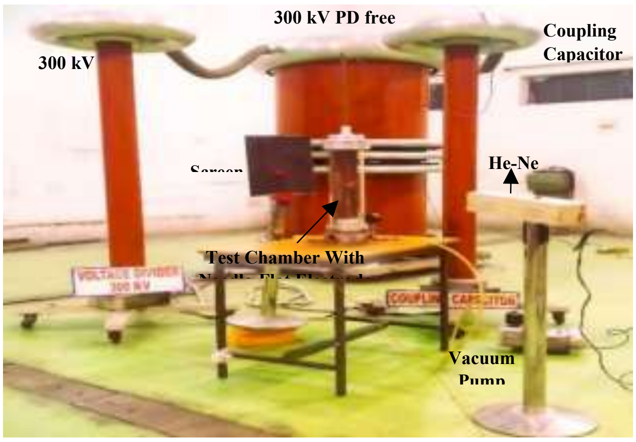

Fig.2. Laboratory setup for Experiment

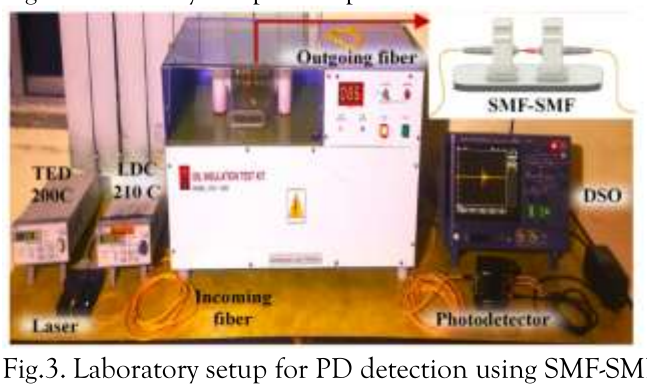

Fig.3. Laboratory setup for PD detection using SMF-SMF coupling-based optical fiber sensor.

In the laser speckle–based optical system, a continuous-wave Helium-Neon (HeNe) laser (wavelength = 632.8 nm, output power 10 mW, beam divergence ≈ 1 mrad) was used as a coherent light source for the corona detection. The test object, consisting of a needle-flat electrode combination, was placed in the low-pressure vessel for the generation of corona discharge, as shown in Fig. 2. The laser beam is directed to the vicinity of discharge sources, guiding the beam path safely. The laser source and detectors were mounted on an anti-vibration optical bench to minimize spurious intensity fluctuations caused by mechanical noise. The necessary shielding was provided to ensure the isolation of the optical system from electromagnetic transients associated with discharge pulses generated in the low-pressure vessel. The laser beam was focused to a spot size of approximately 2 mm and directed towards the screen through the vicinity of the test object surface. Discharge activity within the low-pressure chamber with a needle-flat electrode arrangement generates localized micro-acoustic pressure waves and surface vibrations, which induce temporal variation in the speckle field of laser light, which was captured for PD detection.

Two distinct detection schemes were employed in the first part of the experiment to acquire the data in this work. In the first scheme, a Raspberry Pi-based CMOS camera module was used to capture the two-dimensional speckle pattern evolved from the carona acoustic wave modulated laser beam for frame-to-frame correlation analysis. In this scheme, the PRPD pattern for the standard method and the speckle pattern from the proposed method are recorded in synchronisation for further analysis.

In the second scheme, to identify the intensity modulation caused by the discharge-generated acoustic waves, the speckle field was projected to a silicon photodiode-based optical power sensor (PD 10) designed for free-space light measurements with an aperture size of 10mm and a 400-900 nm spectral range. The photodiode output was amplified using a trans-impedance amplifier and directly connected to the oscilloscope for time-resolved analysis of discharges.

In this scheme, the acquired pulses were synchronized with the electrical PD detection unit through a common trigger system to ensure time synchronization between the proposed detection and electrical detection.

During the experiments, the applied voltage was gradually increased until the PD inception voltage (PDIV) was reached on the lines of standard IEC 60270.

The combined arrangement thus enabled comparison and cross-verification of PD activity through two independent modes, i.e., the conventional PD detection by electrical method on the lines of IEC 60270 and the non-contact laser speckle technique, a new innovative method for PD detection.

Taking inspiration from the above work, instead of a direct laser speckle–based optical system, a fiber-guided sensing module is introduced in the second part of the experiment to assess the effect of an acoustic wave on laser propagation in a medium.

In this experiment, a continuous-wave source, comprising a fiber-coupled pigtailed laser diode (LPS-1550-FC) with a 1.5 mW optical power output and 1530 nm - 1590 nm wavelength, mounted on a laser diode mount (LM9LP), was launched into a single-mode fiber (SMF). The output end of the incoming SMF was aligned with another SMF (outgoing) in free space to establish a fiber-to-fiber coupling path for capturing the demodulated laser signals influenced by the PD source in the test object, as shown in Fig. 3. The free-space coupling distance was maintained at .5 to 1 millimeters to allow interaction with the surrounding medium. The average optical coupling efficiency under quiescent conditions was ~55%. An arrangement, i.e., a needle-flat electrode combination in a test cell, is excited by high voltage, causing generation of acoustic waves resulting in refractive index perturbations of the medium, affecting the coupling efficiency of the SMF-SMF configuration kept in the near vicinity, modulating the laser beam passing through the medium. The modulated light as collected by the other part of the SMF is guided to an amplifier-coupled InGaAs PIN photodetector (PDB480C-AC) having a bandwidth of DC to 3 MHz with very low coupling losses at operating wavelength of 1200 nm - 1700 nm, followed by a transimpedance amplifier. The output from the photodiode is connected to an oscilloscope (DPO4032), having an analog bandwidth (-3 dB) of 350 MHz with a maximum sample rate (all channels) of 2.5 GS/s. Finally, the recorded data is used to plot the detected discharge signals in the time domain and generate the corresponding PRPD pattern. The detected pulses from the proposed method are compared with the pulses obtained from the standard detection technique under similar operating conditions for further analysis and understanding.

IV. RESULTS AND DISCUSSIONS

Following all the schemes discussed above, the applied voltage gradually increased until the PD inception voltage (PDIV) was reached to study the PRPD and speckle pattern.

In the first part of the experiment, as described in the previous section, PRPD and laser speckle patterns are recorded at the voltage levels of 11.2 kV, 23.8 kV, and 37.5 kV at NTP as well as low atmospheric pressure. It is observed that discharge activities in any electrical infrastructure exhibited a strong dependence on applied voltage and its surrounding pressure.

It is profoundly observed from Fig. 4 and Fig. 5 that at NTP as well as low pressure, as the voltage increases, the PD-generated acoustic field becomes stronger and more coherent, causing more photon paths to interfere constructively at the center. This enhances the intensity of the central white region, while the intensity of the red speckle regions diminishes simultaneously due to destructive interference. The effect indicates that the acoustic pressure is coupling efficiently to the optical field, causing energy redistribution that aids the central bright spot rather than the periphery. In short, with rising voltage, the system shows constructive dominance, where the white region grows progressively while the red halo diminishes.

It is evident from Fig. 4 (a) that at normal temperature pressure (NTP), and for a voltage level of 11.2 kV, the speckle contrast remained comparatively low at 11.2 kV with only ~ 0.3 – 2% of pixels reaching the bright-white intensity level and ~ 5–18% occupying the red mid-intensity range, consistent with localized micro-discharges. The corresponding PRPD plots showed limited activity at the same voltage level, typically 2–7 pulses per half-cycle confined to narrow phase windows of ~ 51°– 116° around the negative maximum, with apparent charge magnitudes in the range of 30 – 100 pC and rarely exceeding 100 pC. It is easily followed from Fig. 4 (b) and (c) that with development in voltage, at 23.8 kV and 37.5 kV, the constructive interference strengths and the bright white region enhance with fading of the red halo, while in the standard method, the phase spread and magnitude of the PD events increase as observed from the PRPD pattern.

By contrast, at room temperature of 27°C, with a pressure of 300 mmHg, and applied voltage of 11.2 kV, the rapid intensification of discharge activity was observed where speckle contrast values increased to 0.30 – 0.65 (typical 0.45), with 1.5 – 7% white pixels and 12 – 30% red pixels, reflecting highly dynamic and spatially extended scattering regions. PRPD plots also revealed 8 – 15 pulses per half-cycle distributed over ~ 44°– 133° of the phase angle, with mean apparent charges of 60 – 200 pC, which is a nature of streamer-type discharges as shown in Fig. 5 (a). At low atmospheric pressure with high voltage levels of 23.8kV and 37.5 kV, comparatively more intensification and spread of the bright white area in the speckle pattern can be observed than at NTP with similer voltage level, which is consistent with the wider

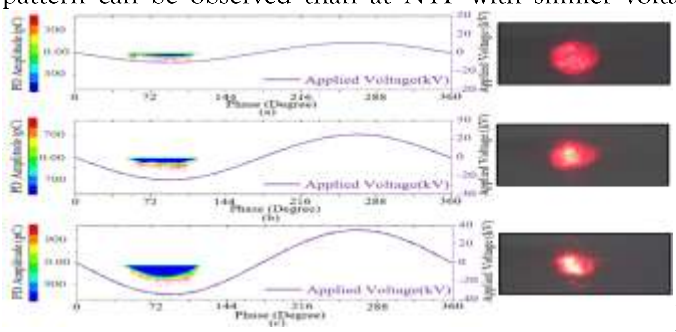

]

Fig.4. PRPD and Speckle pattern for discharge at the voltage levels of (a) 11.2 kV (b) 23.8 kV and (c) 37.5 kV in NTP.

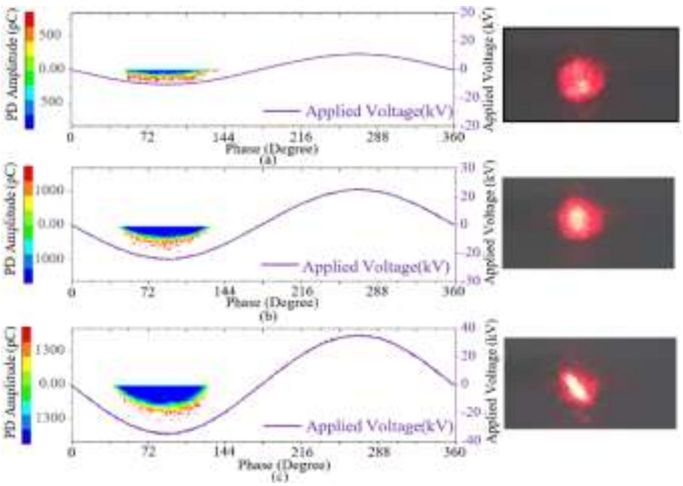

Fig.5. PRPD and Speckle pattern for discharge at the voltage levels of (a) 11.2 kV (b) 23.8 kV, and (c) 37.5 kV in 300 mm-Hg of atmospheric pressure.

International Journal of Environmental Sciences
ISSN: 2229-7359
Vol. 11 No. 24s, 2025
https://www.theaspd.com/ijes.php

spread and bigger magnitude of PD events seen in the PRPD pattren as shown in Fig. 5 (b) and (c). These results confirm that at higher pressure, avalanche development is quenched and discharges remain localized, while at reduced pressure, the longer mean free path promotes efficient avalanche multiplication, leading to higher pulse counts, broader phase distributions, and significantly larger apparent charge magnitudes. This condition clearly favored more frequent and spatially extended streamer discharges, as confirmed by the agreement between speckle imaging and PRPD diagnostics.

In the second part of the experiment, the all-fiber model comprising SMF-SMF coupling in free space, as mentioned in the previous section, is tested. PD is generated by applying high voltage across the electrode configuration, and the SMF-SMF arrangement is kept in the vicinity. The obtained results are shown in Fig. 6. It is evident from the results that the proposed method detected discharge pulses with a satisfactory signal-to-noise ratio (SNR), and pulses are mostly concentrated in the negative maximum of the supply voltage, as supported by the

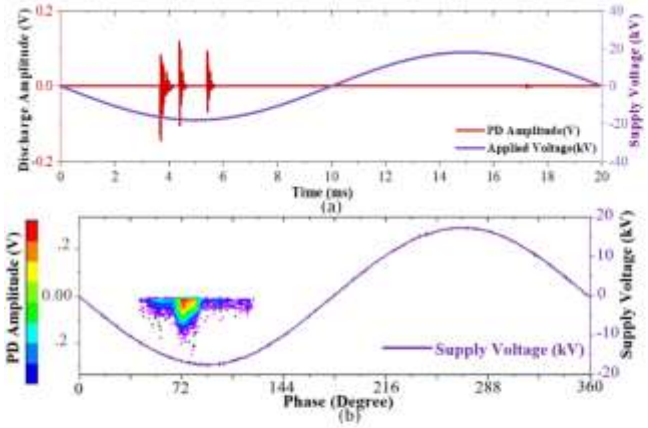

Fig.6. Detection of discharge using the optical fiber-based SMF-SMF sensor and corresponding PRPD for a supply voltage of 18.6 kV.

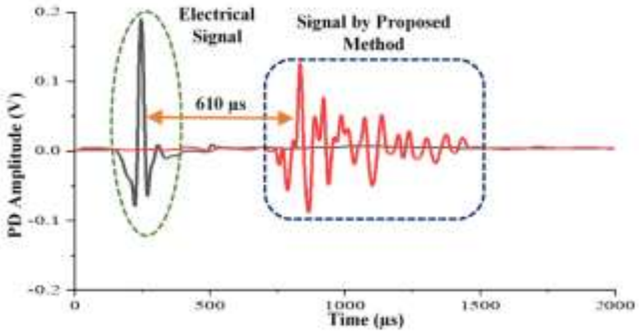

Fig.7. Detected signal using the standard and proposed method.

corresponding PRPD, which is consistent with corona-like discharges.

A comparison study between the pulses detected by conventional electrical PD detection and the proposed acoustic-based optical detection method was conducted to assess compliance with the proposed method. It is observed that the electrical signal exhibited fast-rising pulses with a pulse duration of 64 µs and an amplitude of ~ 200 mV, directly reflecting the discharge current, as shown in Fig. 7. In contrast, it is observed that the optical signals had slower rise times and duration of 746 µs, predominantly in kHz frequency range, corresponding to the acoustic propagation and photoelastic modulation. Despite the temporal broadening, a one-to-one correlation between electrical PD pulses and optical signals was observed with an acquisition delay of 610 µs caused by the propagation of the acoustic wave in air. The proposed acoustic-opto approach provides a non-contact alternative to the conventional PD detection; it effectively senses PD occurrence via secondary acoustic effects, making it suitable for environments where conventional electrical access is difficult, such as aircraft operating in high altitudes.

V. CONCLUSION

The present work demonstrates that laser speckle imaging is a reliable and effective technique for corona discharge diagnostics. Unlike conventional PD detection, which requires a complex laboratory environment, electrical connections, and signal processing, the speckle method is purely optical and non-intrusive, eliminating interference with the complex test circuit. The results establish that the speckle fluctuations strongly correlate with the discharge activity, confirming that optical scattering carries direct information about corona discharges.

The variation in the speckle pattern is vivid with the increase in voltage. At lower pressure, the enhanced speckle dynamics clearly showed more discharge activity. At normal pressure, the fluctuations were limited, which is consistent with the discharge behavior. This shows that the method is sensitive to both the voltage and pressure conditions. The optical fiber-based SMF-SMF arrangement produces a convenient, cost-effective approach for online, onsite corona discharge detection with high reliability. Such advancement will help in insulation optimization and voltage regulation in different sensitive applications, especially under low-pressure conditions, such as aircraft, to reduce the risk of corona-related problems by taking into account the changed discharge characteristics and greater susceptibility to flashover that comes with low-pressure conditions. This will improve maintenance practices and ensure sound operation of electrical assets.

REFERENCES

[1] B. Pinnangudi, R. S. Gorur and A. J. Kroese, "Quantification of corona discharges on nonceramic insulators," in *IEEE Transactions on Dielectrics and Electrical Insulation*, vol. 12, no. 3, pp. 513-523, June 2005, doi: 10.1109/TDEI.2005.1453456.

[2] J. S. N'cho and I. Fofana, "Review of fiber optic diagnostic techniques for power transformers," *Energies*, vol. 13, no. 7, p. 1789, Apr. 2020.

[3] A. Subramaniam, A. Sahoo, S. S. Manohar, S. J. Raman, and S. K. Panda, "Switchgear condition assessment and lifecycle management: Standards, failure statistics, condition assessment, partial discharge analysis, maintenance approaches, and future trends," *IEEE Elect. Insul. Mag.*, vol. 37, no. 3, pp. 27–41, May 2021.

[4] Z. Anane, A. Bayadi, K. Huang, "Distortion phenomena on transmission lines using corona modeling ATP/EMTP ", *IEEE Trans. Dielectrics and Electrical Insulation*, vol. 25, no. 2, pp. 383–389, 2018. DOI: 10.1109/TDEI.2017.006484.

[5] I. Christou and I. Cotton, "Methods for partial discharge testing of aerospace cables," in *Proc. IEEE Int. Symp. Electr. Insul.*, San Diego, CA, USA, Jun. 2010, pp. 1–5.

[6] C. Emersic, R. Lowndes, I. Cotton, S. Rowland and R. Freer, "The effects of pressure and temperature on partial discharge degradation of silicone conformai coatings," *in IEEE Transactions on Dielectrics and Electrical Insulation*, vol. 24, no. 5, pp. 2986-2994, Oct. 2017, doi: 10.1109/TDEI.2017.006466.

[7] M. Borghei and M. Ghassemi, "Separation and Classification of Corona Discharges Under Low Pressures Based on Deep Learning Method," *in IEEE Transactions on Dielectrics and Electrical Insulation*, vol. 29, no. 1, pp. 319-326, Feb. 2022, doi: 10.1109/TDEI.2022.3146608.

[8] C. Emersic, R. Lowndes, I. Cotton, S. Rowland, and R. Freer, "Degradation of conformal coatings on printed circuit boards due to partial discharge," *IEEE Trans. Dielectr. Electr. Insul.*, vol. 23, no. 4, pp. 2232–2240, Aug. 2016.

[9] *Partial Discharge Measurements*, Standard IEC 60270, 2015.

[10] J. A. Ardila-Rey, D. Figueroa Karmelic, F. Pizarro, S. Govindarajan, B. Albuquerque de Castro and R. Schurch, "Bioinspired Ultrahigh Frequency Antenna for Partial Discharge Detection in High-Voltage Equipment," in *IEEE Transactions on Instrumentation and Measurement*, vol. 73, pp. 1-18, 2024, Art no. 6007318, doi: 10.1109/TIM.2024.3421437.

[11] Y. Zhang, B. Wang and Q. Yang, "Detection of Discharging Insulators via Acoustic and Visible Image Fusion," in *IEEE Transactions on Instrumentation and Measurement*, vol. 74, pp. 1-12, 2025, Art no. 2542612, doi: 10.1109/TIM.2025.3593549.

[12] H. Liu, J. -m. Li, J. -h. Sun, S. -h. Wang, W. -q. Qin and G. -m. MA, "The Effect of Fluorescent Fiber Optic Arrangement on Partial Discharge Detection Sensitivity in Gas Insulated Switchgear," *2025 10th Asia Conference on Power and Electrical Engineering (ACPEE)*, Beijing, China, 2025, pp. 2721-2725, doi: 10.1109/ACPEE64358.2025.11040908.

[13] Aragão Rodrigues, G., Vinicius Silveira Araujo, B., Herbert Paixão de Oliveira, J., Victor Rocha Xavier, G., Daniel Enes de Souza Lebre, U., Antony Cordeiro, C., Oliveira Freire, E., & Vilela Ferreira, T. (2024). Automated monitoring of insulation by ultraviolet imaging employing deep learning. *Measurement*, *242*, 116018. https://doi.org/10.1 016/j.measurement.2024.116018.

[14] Kang, J., Chae, D., Mun, Y., Park, J., & Lee, B. (2022). Study on the Measurement Technique and Judgment Procedure of Ultrasonic Corona Imaging Equipment. *Energies*, *16*(14), 5529. https://doi.org/10.3390/ en16145529.

[15] J. -R. Riba, Á. Gómez-Pau and M. Moreno-Eguilaz, "Sensor Comparison for Corona Discharge Detection Under Low Pressure Conditions," in *IEEE Sensors Journal*, vol. 20, no. 19, pp. 11698-11706, 1 Oct.1, 2020, doi: 10.1109/JSEN.2020.2998827.

[16] Riba, J. (2019). Experimental Study of Visual Corona under Aeronautic Pressure Conditions Using Low-Cost Imaging Sensors. *Sensors*, 20 (2), 411.

[17] Siebler, D., Rohwetter, P., Brusenbach, R., & Plath, R. (2014). Optical-only Detection of Partial Discharge with Fluorescent Polymer Optical Fiber Sensors. *Procedia Engineering*, *120*, 845848. https://doi.org/10. 1016/j.proeng.2015.08.711.

[18] Kozioł, M.; Nagi, Ł.; Kunicki, M.; Urbaniec, I. Radiation in the Optical and UHF Range Emitted by Partial Discharges. *Energies* 2019, *12*, 4334.

[19] Chen, L.; MacAlpine, J.M.K.; Bian, X.; Wang, L.; Guan, Z. Comparison of methods for determining corona inception voltages of transmission line conductors. *J. Electrostat.* 2013, *71*, 269–275.